Electronic Supplementary Material (ESI) for Dalton Transactions.

Characterization of a meso-chiral hexanuclear Cu(II) cage from chiral inversion of L-alanine Schiff base

C. M. Rajesh and Manabendra Ray*

Department of Chemistry, Indian Institute of Technology Guwahati, Guwahati - 781039, Assam, India.

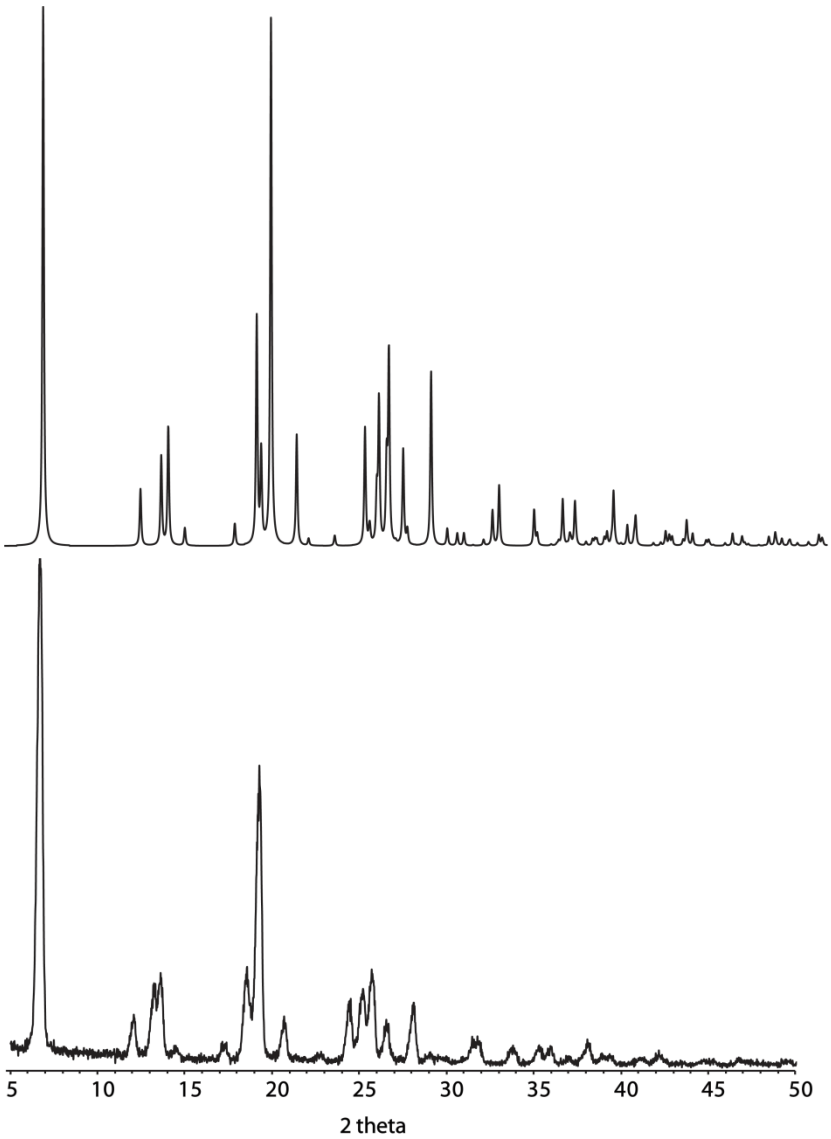

Figure S1. Powder-XRD pattern of LiHL simulated from X-ray structure (above) and experimental pattern (below) from bulk.

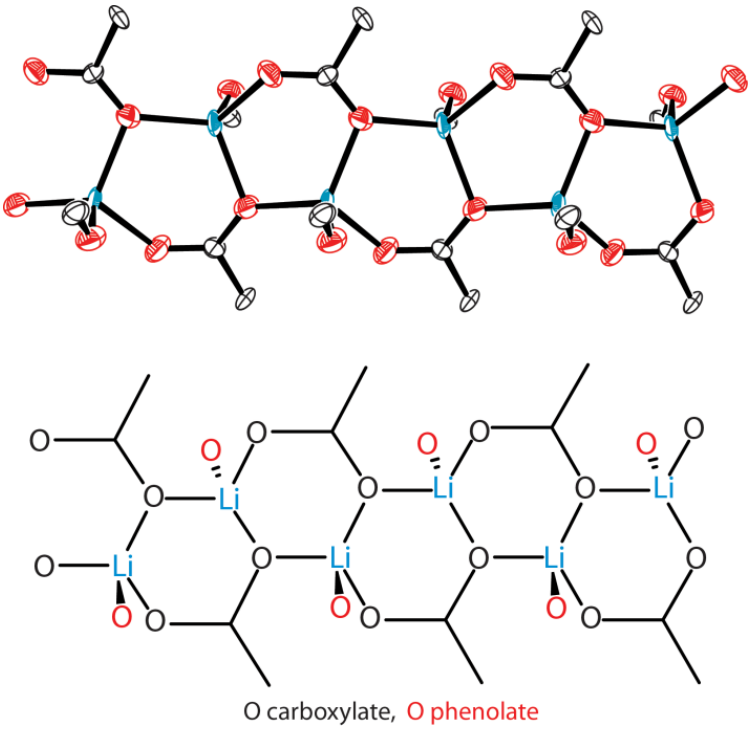

Figure S2. Network formed by the carboxylate and phenolate coordination to -Li^+.

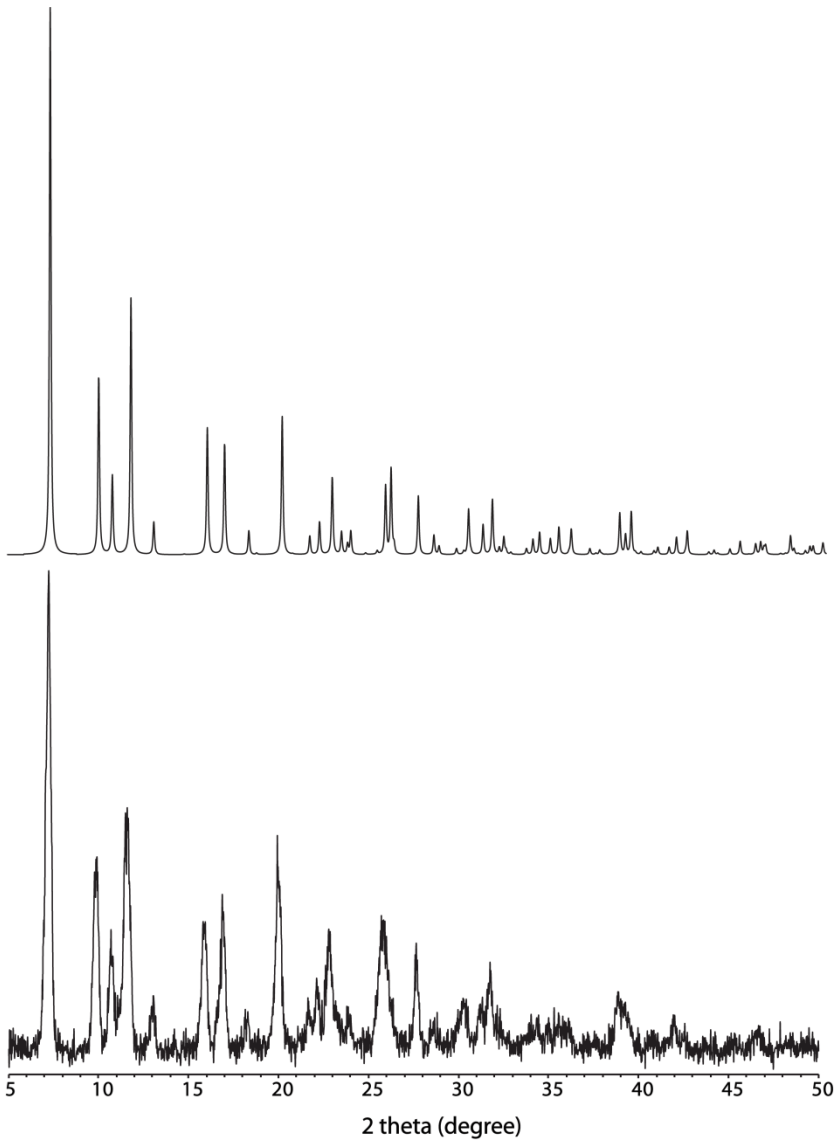

Figure 3a. Powder-XRD pattern of **1** simulated from X-ray structure (above) and experimental pattern (below) from bulk.

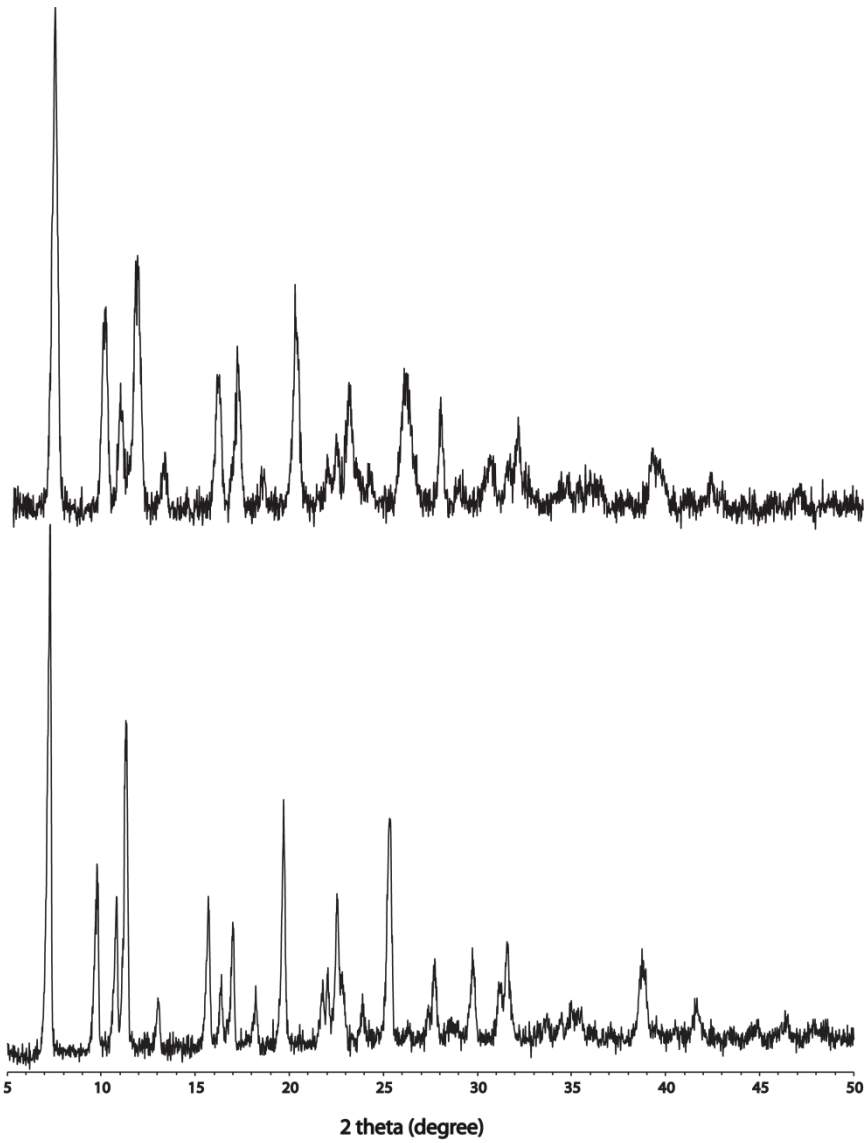

Figure 3b. Experimental Powder-XRD pattern of **1** (above) compared with that of **1a** (below).

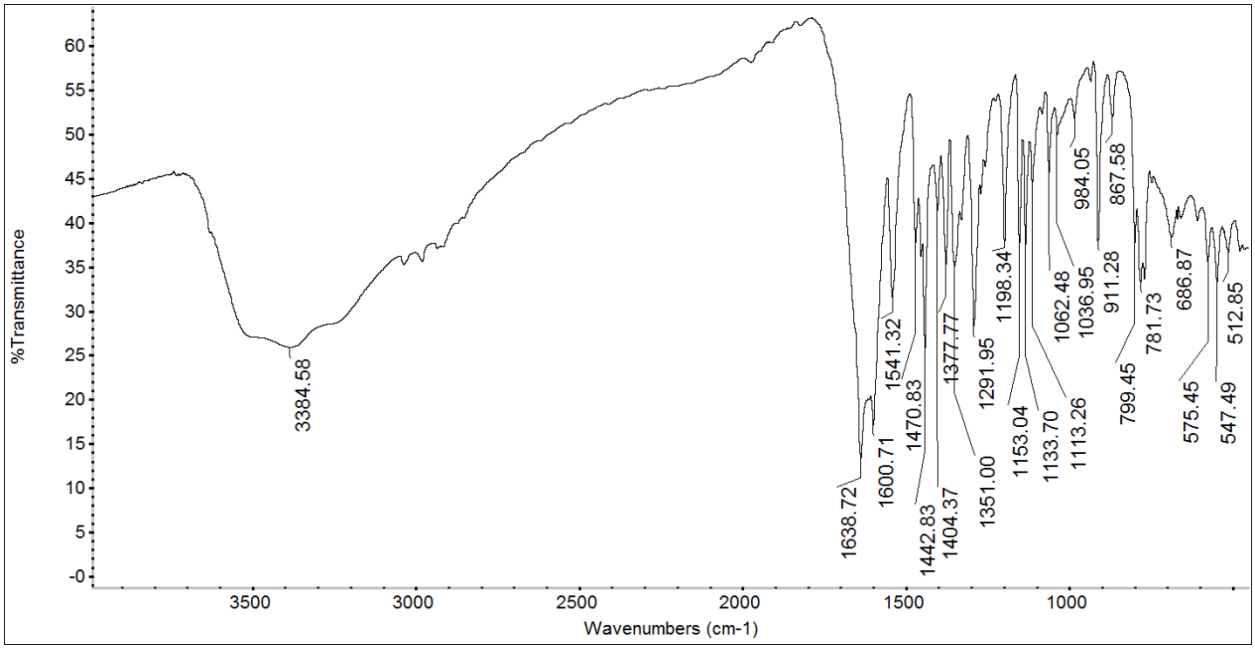

Figure S4a. FT-IR spectrum of **1**.

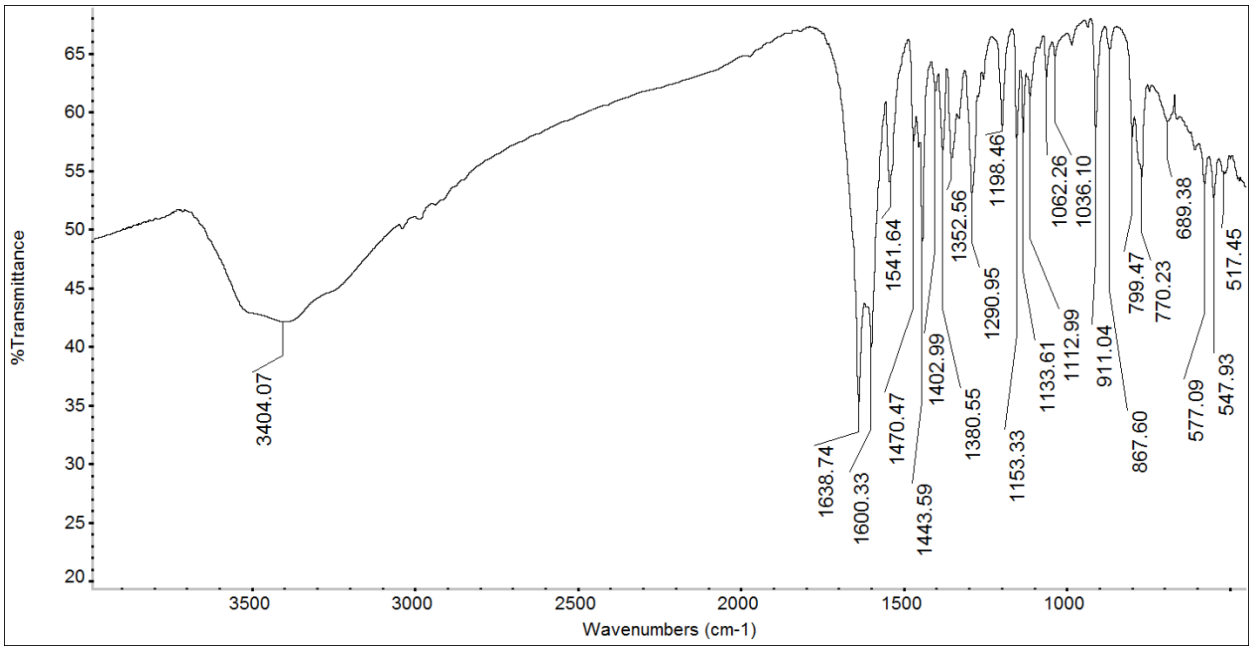

Figure S4b. FT-IR spectrum of **1a**.

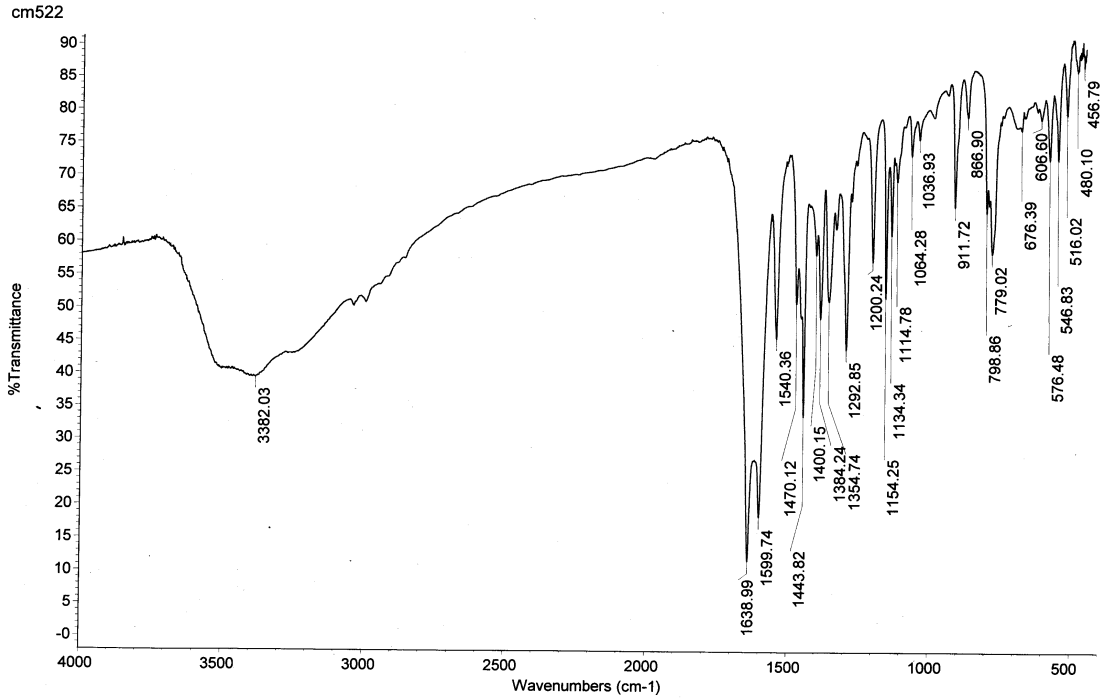

Figure S4c. FT-IR spectrum of **1b**.

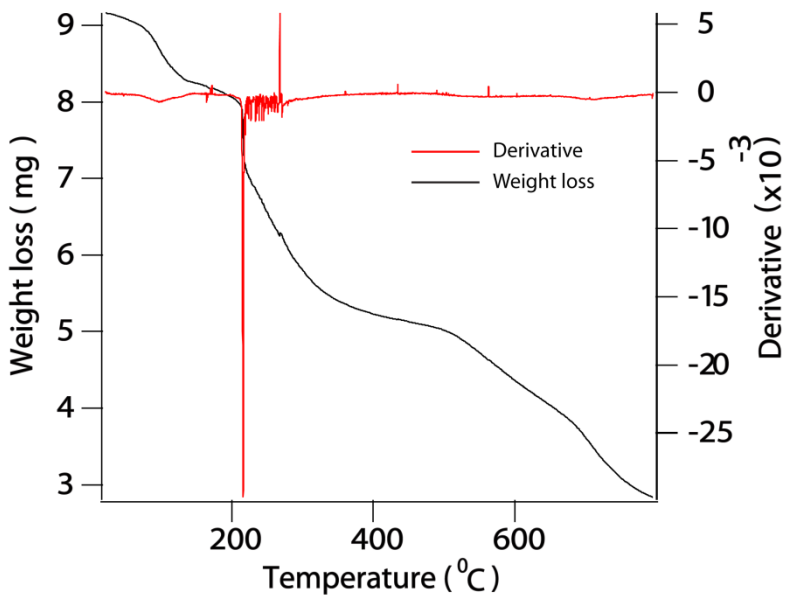

Figure S5a. TGA and DTA plot of **1.**

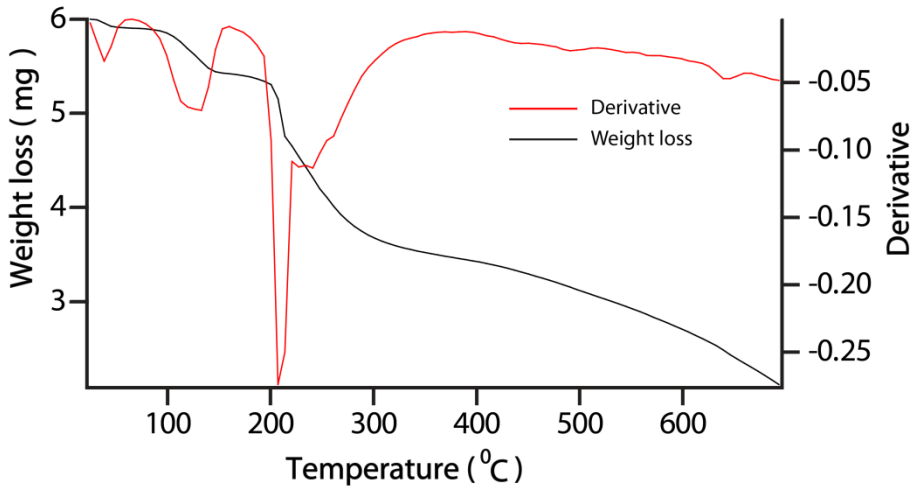

Figure S5b. TGA and DTA plot of **1a.**

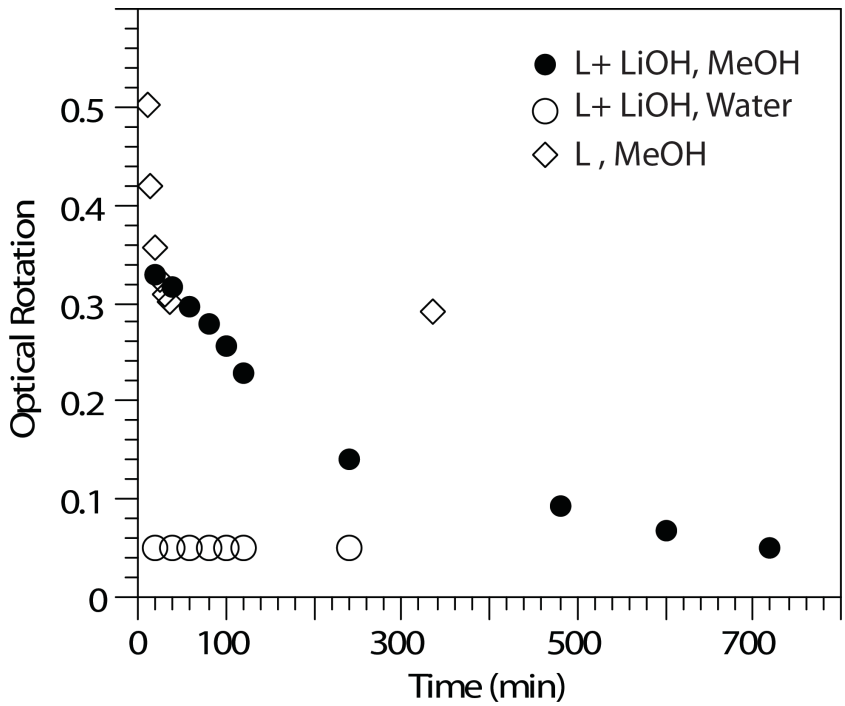

Figure S6. Time vs optical rotation plots (L – LiHL).

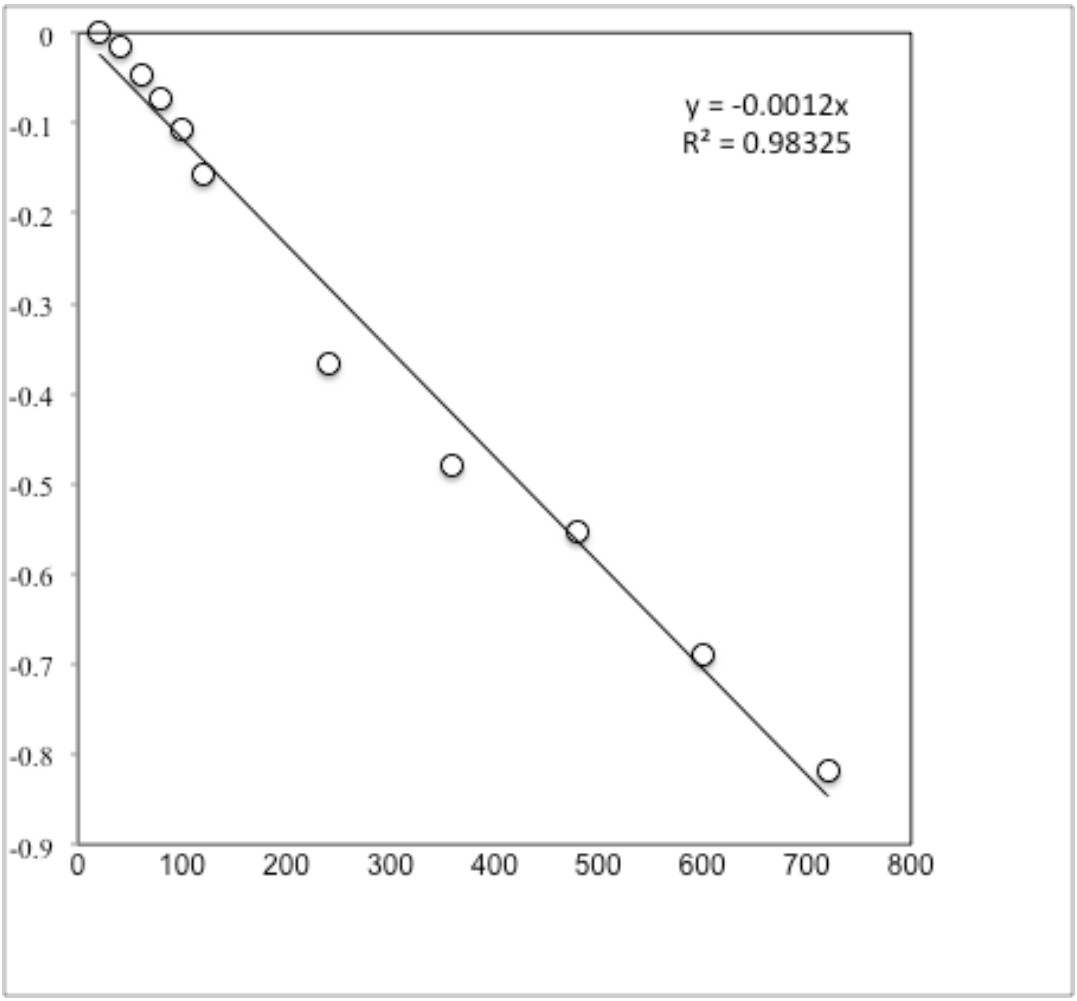

Figure S7. Plot of time in min (X axis) vs log (rotation at t min/initial rotation) (Y axis) for LiHL and 1 equiv. of LiOH in methanol at room temperature.

Note. Kinetic measurements were performed by monitoring the decrease of optical rotation at 589nm over a time period of 12h. Solvent used Methanol. Temperature during measurement 28°C. The time of measurement started at 20 min after the addition of base as the mixing of the base and insertion inside the cell took time. From the data of initial one hour, only 0.015 rotation (4.6% decrease after 20 min). Thus initial time delay should not affect the order of the rate appreciably. Data were plotted using the first order equation as follows:

$$\log\left(\frac{rotation\ at\ t\ \text{min}}{initial\ rotation}\right) = -\left(\frac{k}{2.303}\right)t$$

k_{obs} from plot $2.76\text{x}10^{-3}$ /min

$k_r = k_{obs}/(OH^-) = 0.110\ \text{min}^{-1}\text{M}^{-1}$

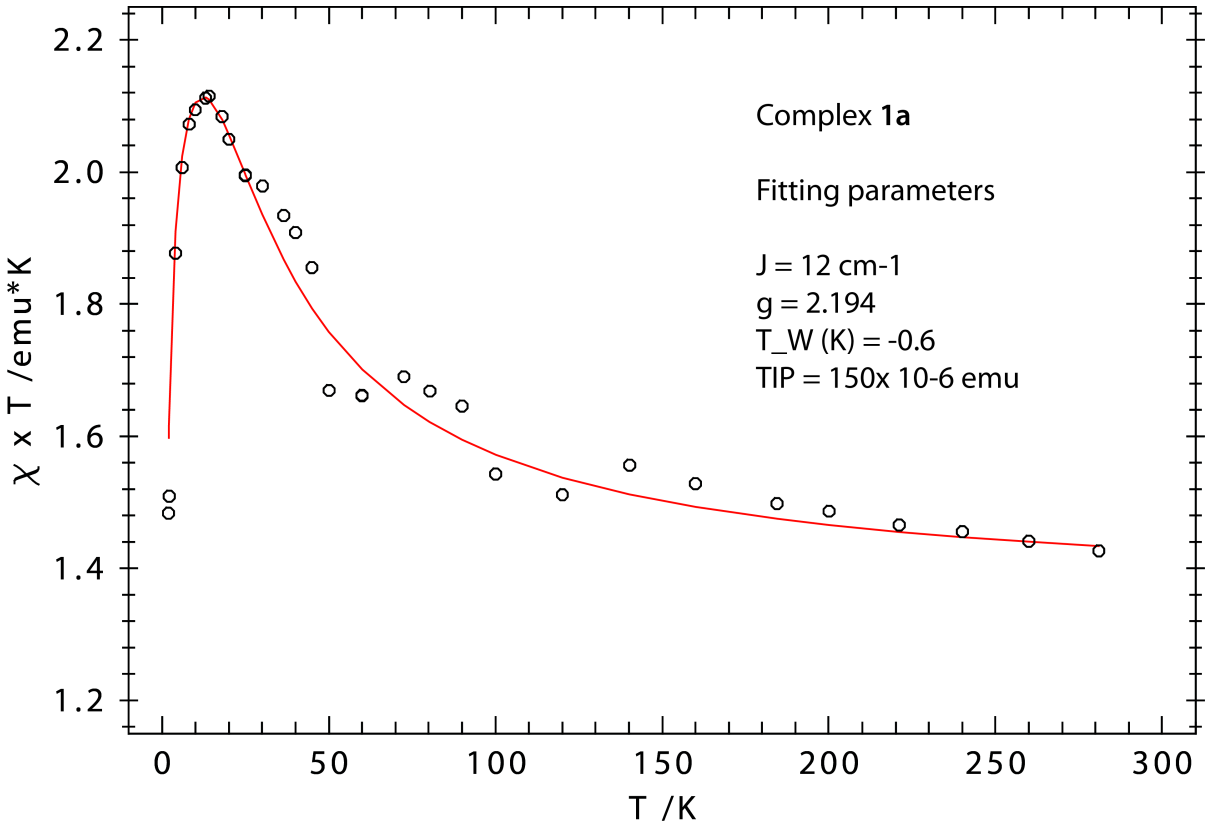

Figure S8. Plot of X_MT vs T in the range 2-300 K for **1a.**

Parameters used:
X_{dia} for Complex 1 = -398×10^{-6} /g atom
FW used: 880.79

X_{dia} for Complex 1a = -396×10^{-6} /g atom
FW used: 881.3

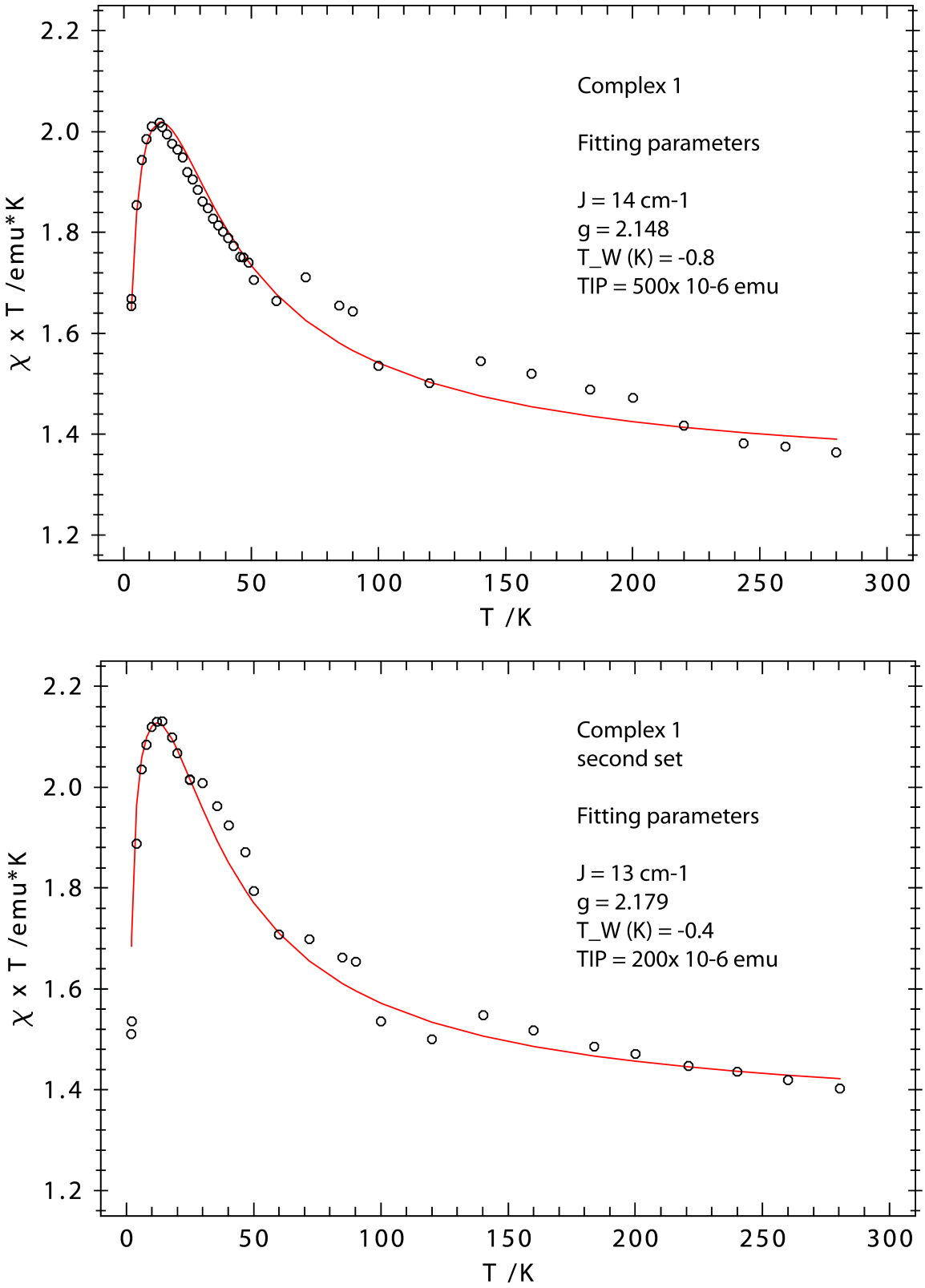

Figure S9. Plot of X_MT vs T in the range 2-300 K for **1.**

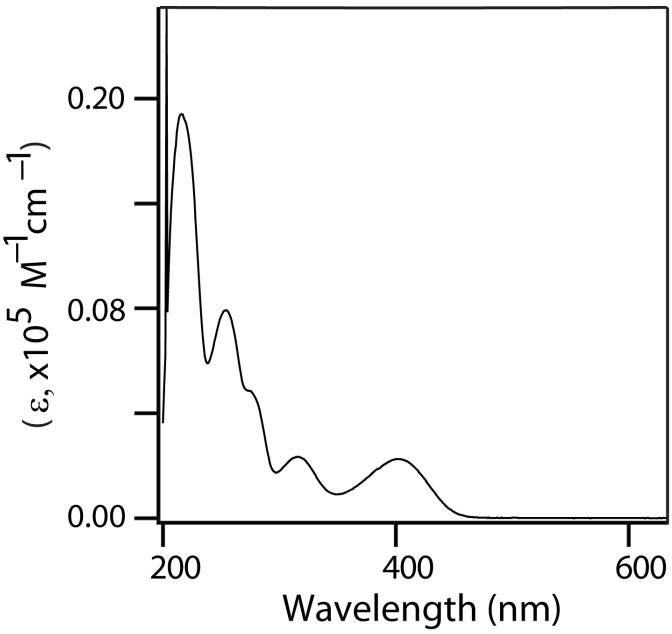

Figure S10. UV-visible spectrum of LiHL (60.0 μM) in MeOH.

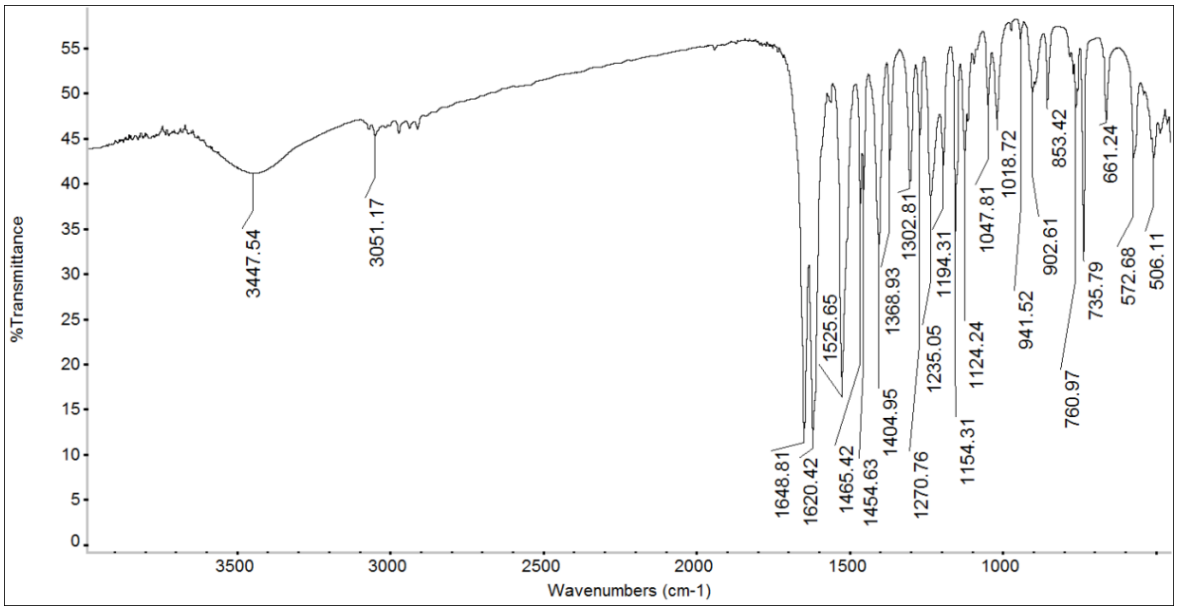

Figure S11. FT-IR spectrum of LiHL.

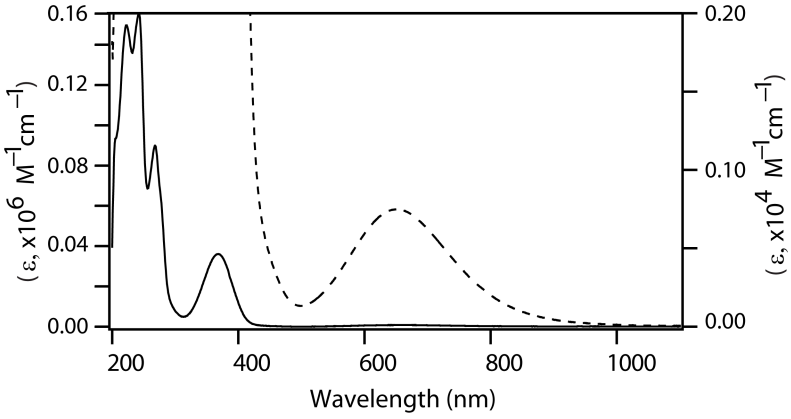

Figure S12. UV-visible spectrum of **1** in MeOH [(- - - - 6.6×10^{-4} M, /Cu_6 unit) and (— 6.6×10^{-6} M, /Cu_6 unit)]

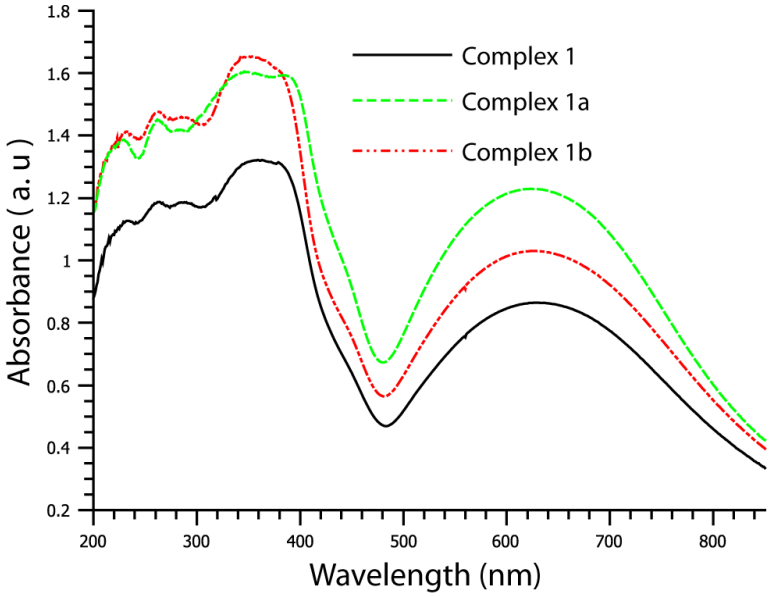

Figure S13. Solid state UV-visible spectrum of **1**, **1a** and **1b.**

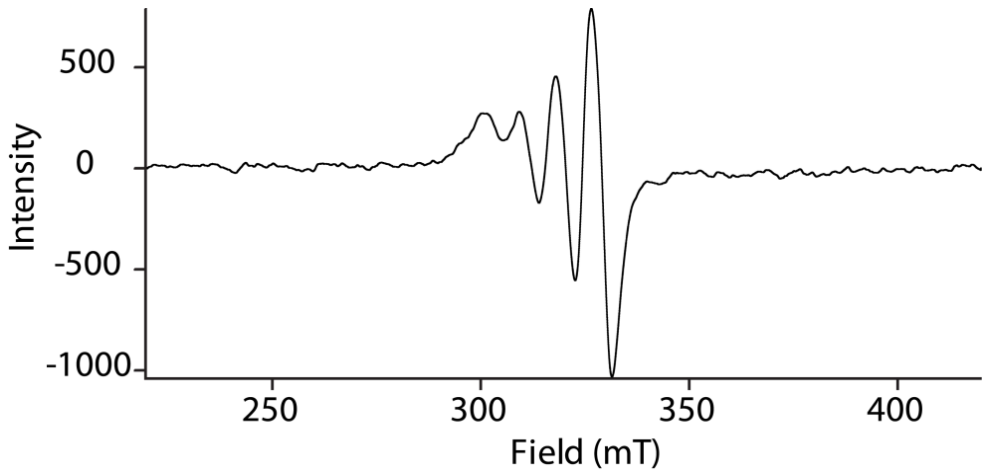

Figure S14a. EPR spectrum of **1** in DMF at 298 K

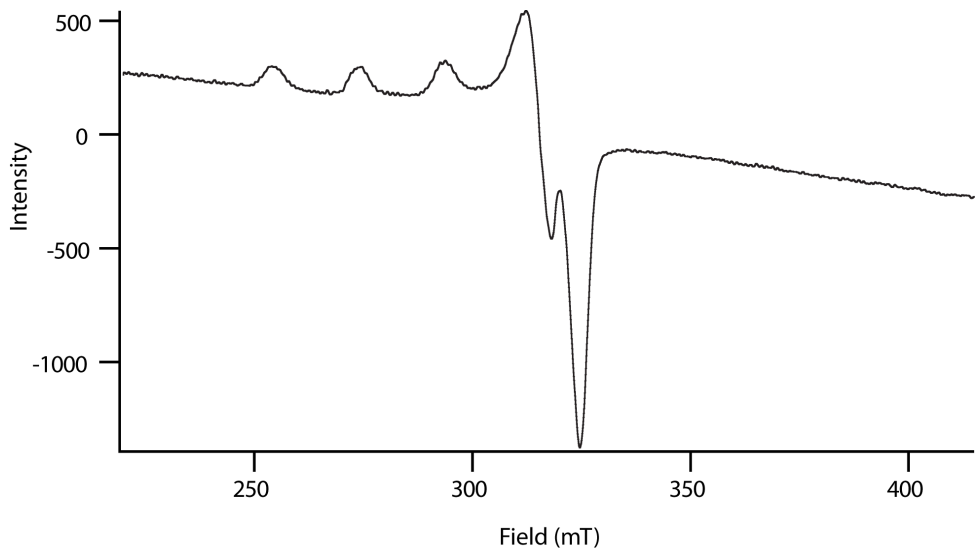

Figure S14b. EPR spectrum of **1** in DMF at 77 K

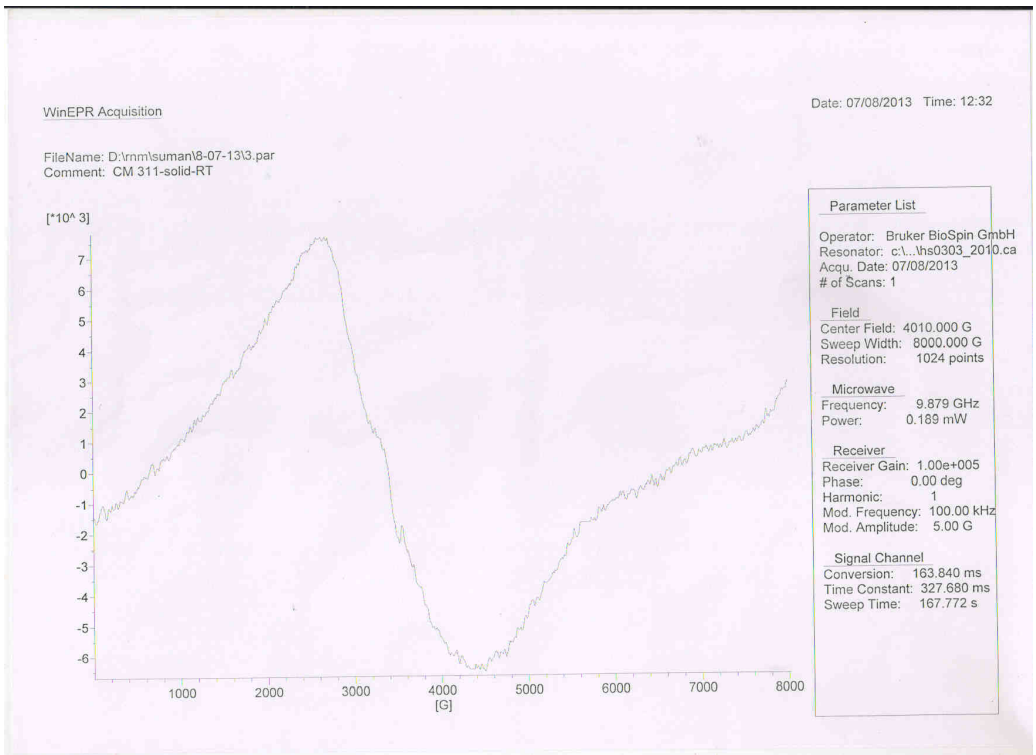

Figure S14c. Solid state EPR spectrum of **1** at 298 K

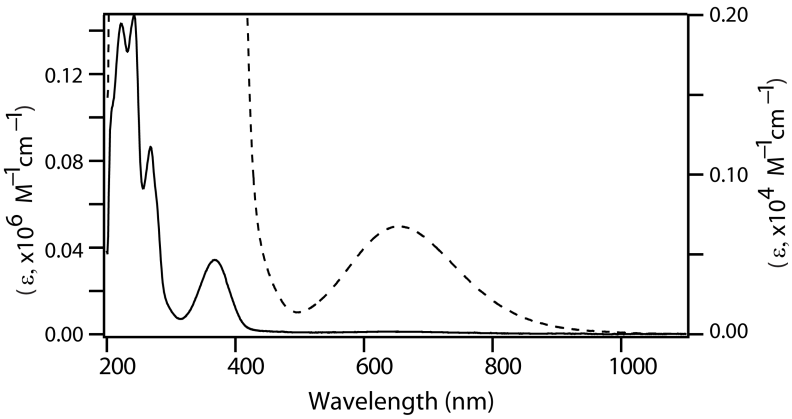

Figure S15. UV-visible spectrum of **1a** in MeOH [(- - - - 6.6×10^{-4} M, /Cu_6 unit) and (— 6.6×10^{-6} M, /Cu_6 unit)]

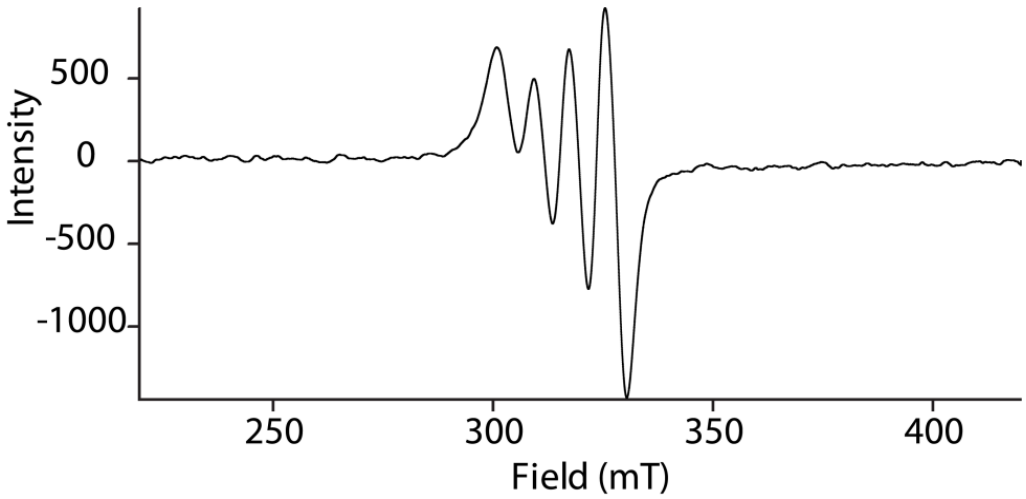

Figure S16a. EPR spectrum of **1a** in MeOH at 298 K.

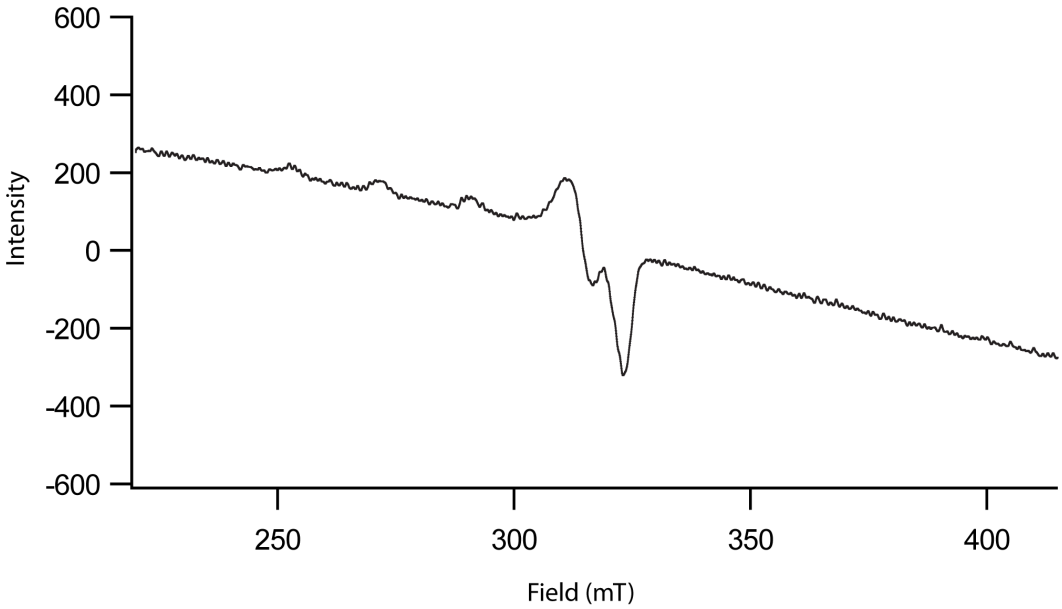

Figure S16b. EPR spectrum of **1a** in MeOH at 77 K

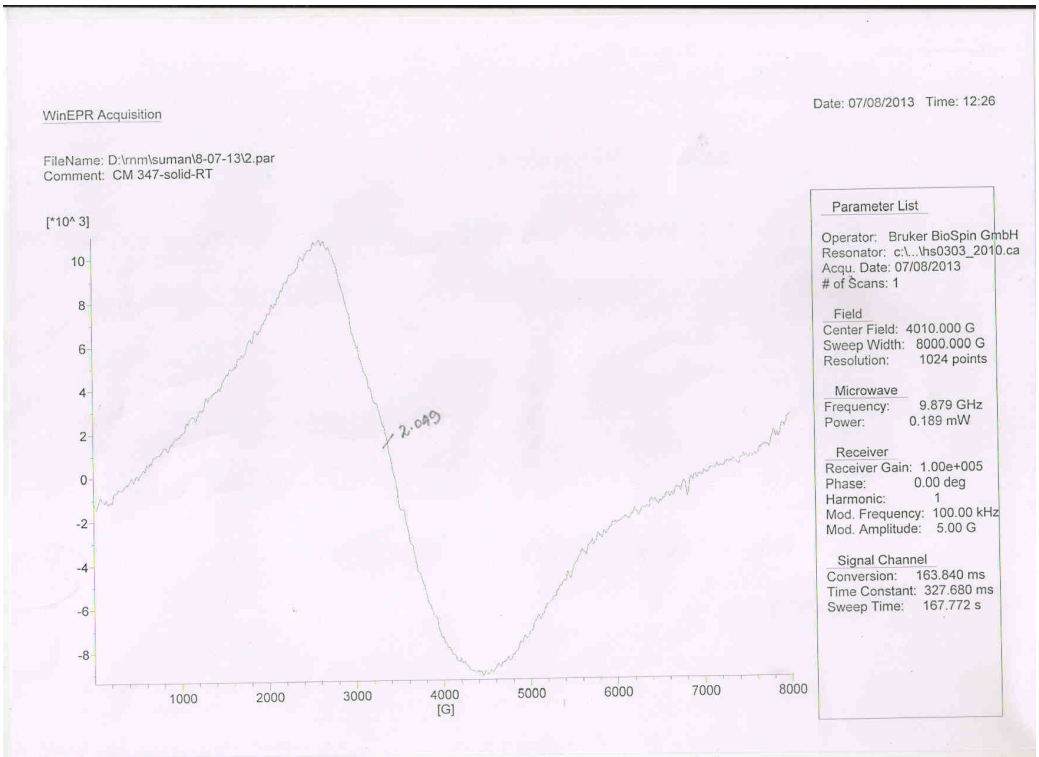

Figure S16c. Solid state EPR spectrum of **1a** at 298 K

Table S1. The actual peak heights of the various non-coordinated oxygen atoms and carbons in the structure of Complex 1 .

Atom label	peak height	Atom label	peak height
O5_i	4.48	C1	4.77
O6_i	4.25	C2	4.67
O7_i	2.01	C3	4.59
		C4	4.89
		C5	5.60
		C6	6.36
		C7	5.49
		C8	5.11
		C9	4.84
		C10	4.86